Physical Communication 60 (2023) 102157

Contents lists available at ScienceDirect

Physical Communication

journal homepage: www.elsevier.com/locate/phycom

Full length article

Deep learning and deep transfer learning-based OPM for FMF systems

M.A. Amirabadi, M.H. Kahaei *, S.A. Nezamalhosseini

School of Electrical Engineering, Iran University of Science and Technology (IUST), Tehran, 1684613114, Iran

ARTICLE INFO

Article history:
Received 8 July 2022
Received in revised form 11 February 2023
Accepted 24 July 2023
Available online 1 August 2023

Keywords:
Deep learning
Deep transfer learning
Optical performance monitoring
Few-mode fiber
Nonlinearity

ABSTRACT

Optical performance monitoring (OPM) is indispensable to guarantee stable and reliable operation in few-mode fiber (FMF)-based transmission. OPM consists of measuring optical phenomena such as generalized signal-to-noise ratio (GSNR) based on analytical models. GSNR comprises nonlinear interference (NLI) noise which can be calculated either by exact analytical models e.g., enhanced Gaussian noise (EGN) model which is accurate but computationally complex, or asymptotic analytical models e.g., closed-form EGN model which are approximate but computationally fast. In this paper, we employ deep learning (DL) as an accurate and fast alternative for OPM in FMF-based transmission. However, DL-based OPM requires a large dataset to achieve proper performance whilst it is very difficult and time-consuming to obtain a large field or synthetic dataset. Regarding this issue, we develop deep transfer learning (DTL) for OPM in FMF to realize a fast response requiring a small training dataset and a few training epochs despite various changes in system/link parameters such as launched power, fiber type, and the number of modes. Results show root mean squared error of GSNR estimation is less than 0.02 dB for DL and DTL-based OPM methods. Compared to DL-based OPM, DTL-based OPM records 3 and 5 times reduction in required training dataset size and the number of epochs, respectively which is beneficial for real-time applications

1. Introduction

Single-mode fiber (SMF) optical communication systems are achieving their nonlinear capacity limits. Few-mode fiber (FMF)-based transmission is a candidate for the next-generation optical networks which enhances capacity by multiplexing parallel data streams utilizing different spatial modes [1–4]. FMF systems suffer from FMF linear and nonlinear effects. The FMF linear impairments include attenuation, dispersion (chromatic and modal), and linear coupling [5–9]. The linear coupling between modes results in a power transfer from one mode to another mode [6]. Weak coupling appears in short-range links [10,11] while the strong coupling is more prone in long-range links [6,8]. In weak coupling, each mode is processed separately without using complex Multiple-Input Multiple-Output (MIMO) Digital Signal Processing (DSP) [11] while in strong coupling MIMO DSP is required to compensate FMF linear effects [5]. MIMO DSP complexity is low in nearly equal group delays between the propagating modes [12–15], and minimum differential mode group delay can be obtained by Graded index fibers with a nearly parabolic index profile [7]. FMF nonlinear interactions include Kerr-based nonlinear effect and nonlinear coupling [13–19].

FMF-based transmission is known for increased transparency and data rate, these systems are accompanied by transmission margins requiring the physical layer fault management capability. This in turn collects attention focusing on optical performance monitoring (OPM) as an important tool for managing FMF systems in applications such as amplifier gain control, signal health evaluation, fault management, and mode identification [20]. OPM assesses the signal quality by evaluating optical phenomena such as the generalized signal-to-noise ratio (GSNR) or physical characteristics including chromatic dispersion (CD), and polarization mode dispersion (PMD) without directly measuring the transmitted signal sequence. GSNR estimation can be formulated in terms of amplified spontaneous emission (ASE) noise and nonlinear interference (NLI) noise [20]. The ASE noise calculation is simple, while the NLI noise computation is challenging.

FMF NLI noise can be predicted by solving the Manakov equation [8] using the split-step Fourier method (SSFM) through many successive numerical simulation steps. SSFM method has good accuracy along with computational complexity. By taking into account the first-order perturbation approximation [21] while solving the Manakov equation, the Gaussian noise (GN) model [7,21] and enhanced GN (EGN) model [4,22,23] predict the NLI noise with lower complexity compared with SSFM method. The GN model considers Gaussian distribution for the transmitted signal while the EGN model takes into account the modulation format effect. The computational complexity of integral-form GN

* Corresponding author.
E-mail addresses: m_amirabadi@elec.iust.ac.ir (M.A. Amirabadi), kahaei@iust.ac.ir (M.H. Kahaei), nezam@iust.ac.ir (S.A. Nezamalhosseini).

https://doi.org/10.1016/j.phycom.2023.102157
1874-4907/

Table 1
Comparison between different works on DL/DTL for OPM in SMF and FMF systems.

Ref.	SMF/ FMF	DL/ DTL	Algorithm	Labels	Features	Performance	Year	Complexity analysis
[32]	SMF	DL	ANN	OSNR, CD, and PMD monitoring	AH	RMSE of OSNR monitoring 0.1 dB	2012	No
[33]	SMF	DL	ANN	MFI, OSNR and NLI noise power monitoring	ACH	RMSE of OSNR monitoring 0.37 dB	2021	No
[34]	SMF	DL	ANN	Fiber nonlinear noise to signal ratio monitoring	Amplitude noise covariance	Monitoring error 0.6 dB	2017	No
[35]	SMF	DL	DNN	OSNR monitoring	AH	RMSE of OSNR monitoring 0.2 dB	2018	No
[36]	SMF	DL	DNN	MFI	AH	Accuracy of MFI 100%	2016	No
[37]	SMF	DL	CNN	MFI	AAH	Accuracy of MFI 100%	2020	No
[38]	SMF	DL	CNN	OSNR monitoring	AH	RMSE of OSNR monitoring 0.246 dB	2021	No
[39]	SMF	DL	CNN	MFI and OSNR monitoring	AH	Accuracy of OSNR monitoring 97.6%	2021	No
[40]	SMF	DL	RNN	Joint OSNR and NLI noise power monitoring	Frequency domain features of the input signal	Error of OSNR monitoring 1.0 dB	2018	No
[41]	SMF	DL	RNN	Joint OSNR and CD monitoring	AAH	RMSE of OSNR monitoring 0.5 dB	2023	No
[42]	SMF	DTL	DNN	OSNR monitoring	AH	RMSE of OSNR monitoring 0.1 dB	2019	No
[30]	SMF	DTL	DNN	MFI and OSNR monitoring	AH	RMSE of OSNR monitoring 1.09 dB	2020	No
[31]	SMF	DTL	CNN	Multi-impairment diagnosis	Eye diagram	Accuracy 99.88%	2019	No
[43]	FMF	DL	ANN	MFI	ACH	Accuracy of MFI 98%	2019	No
[44]	FMF	DL	ANN	OSNR, CD, and mode coupling monitoring	ATDH	RMSE of OSNR monitoring 0.0015 dB	2022	No
[45]	FMF	DL	CNN	OSNR, CD, and mode coupling monitoring	ACH	Accuracy of OSNR monitoring 90%	2021	No
[46]	FMF	DTL	DNN	MFI and OSNR monitoring	Signal constellation	RMSE of OSNR monitoring 0.1 dB	2022	No
[47]	FMF	DTL	CNN	MFI	Signal constellation	Accuracy of MFI 97.8%	2021	No
This work	FMF	Both	DNN	GSNR estimation	System/link parameters	RMSE of GSNR monitoring 0.02 dB	2023	Yes

and EGN formulations makes them improper for real-time applications. In contrast, closed-form GN and EGN models are fast but only applicable to rectangular-shaped Nyquist wavelength division multiplexing (WDM) with channel spacing close to symbol rate [22,24]. Deep learning (DL) has been presented as a quite fast and accurate method to predict NLI noise [20]. DL-based OPM can be trained in a supervised manner to find out the relationship between the observed GSNR at the receiver and the link configuration in terms of system/link parameters such as transmitted power, link length, number of spans, and ASE noise. However, efficient deployment of DL-based OPM algorithms needs a large dataset while generating a large field/synthetic dataset based on FMF transmission is very difficult and time-consuming [25,26]. Besides, in case the FMF system/link conditions change, a lot of new training samples should be added and the DL algorithm should be re-trained to manage the correct OPM operation [27–29]. In this context, deploying deep transfer learning (DTL) in OPM, as a special DL implementation, can reduce required training samples/epochs by adjusting hyperparameters of the DL algorithm based on prior knowledge rather than random initialization [30]. In other words, DTL deploys hyperparameters obtained while training the DL algorithm based on the source dataset as the starting point for training the DNN based on the target dataset [31].

1.1. Literature review

DL/DTL has recently appeared as a fast and accurate solution for OPM in SMF systems while applying DL/DTL for OPM in FMF systems is still in its infancy. Table 1 summarizes the literature on DL/DTL-based OPM for SMF and FMF systems, in the following, we review these works by dividing them into four categories.

DL-based OPM for SMF: In [32], artificial neural network (ANN) is applied for the joint optical signal-to-noise ratio (OSNR), CD, and PMD monitoring using asynchronously histograms (AHs). In [33], authors employed ANN for joint modulation format identification (MFI), OSNR, and NLI noise power monitoring using asynchronous complex histogram (ACH) features. ANN also is deployed in [34] to monitor fiber nonlinear noise-to-signal ratio based on amplitude noise covariance of received symbols. Deep neural network (DNN) is trained in [35,36] by using AH features to monitor the OSNR and MFI, respectively. Convolutional neural network (CNN) is applied in [37] for MFI in SMF elastic optical networks (EONs) considering asynchronous amplitude histogram (AAH) features. In [38,39], authors employed CNN respectively for OSNR monitoring and joint OSNR monitoring and MFI using AH features. The long short-term memory network is utilized in [40] for joint OSNR and NLI noise power monitoring using frequency domain features of the input signal and in [41] for joint OSNR and CD monitoring based on AAH features.

DTL-based OPM for SMF: Authors of [42] and [30] experimentally demonstrated DNN-based DTL for OSNR monitoring and joint OSNR monitoring and MFI using AH features, respectively. DTL is employed in [31] for multi-impairment diagnosis based on eye-diagram features.

DL-based OPM for FMF: In [43], ANN is applied for MFI in FMF EONs using features extracted from the ACHs. Authors of [44] and [45], respectively considered ANN and DNN for joint OSNR, CD, and mode coupling monitoring in FMF networks using asynchronous tap delay histogram (ATDH) and ACH features.

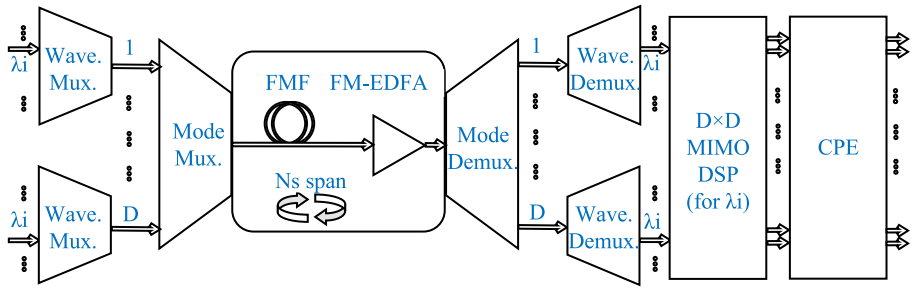

Fig. 1. Schematic diagram of considered FMF link.

DTL-based OPM for FMF: Authors of [46] employed DNN-based DTL in FMF EONs using signal constellation features for joint OSNR monitoring and MFI. In [47], a CNN-assisted DTL approach is applied for MFI in FMF EONs.

1.2. Motivations, novelties, and contributions

FMF-based transmission is encountered with additional impairments to SMF, e.g., modal dispersion, mode-dependent attenuation/gain, and linear/nonlinear coupling. FMF linear effects are compensated by the MIMO DSP, however, these effects consistently affect the FMF nonlinear effects. These impacts along with the nonlinear coupling are the FMF nonlinearity specificities. Therefore, the trained DL/DTL models for SMF systems are not functional in the FMF case the model should be re-tuned and re-trained considering these specifications. The potential development of FMF-based transmission in future optical networks necessitates investigating the applicability of DL/DTL-based OPM or FMF systems. Despite this importance, few works are available in this regard. Besides, there is a lack of complexity analysis to show the complexity-performance trade-off considering the DL/DTL-based OPM method and the well-known conventional approaches.

In this paper, we present and develop DL and DTL-based regressors for OPM in FMF-based transmission. In the DL-based approach, we utilize physical layer parameters as the features and the GSNR (calculated by the EGN model) as the label. To test the feasibility of the proposed DTL-based method, we change the FMF type, launch power, and the number of modes. The novelties and contributions of this paper are as follows

- Presenting DL and DTL-based approaches for OPM in FMF-based transmission, successfully estimating the OSNR within 0.02 dB of the root mean squared error (RMSE).
- Designing DTL-based method for OPM in FMF systems, working efficiently even with small training dataset and few training epochs despite a huge change in system/link parameters while transfer learning compared with re-training, reducing the required training samples and epochs respectively 3 and 5 times and providing 0.02 dB RMSE using 100 points training dataset.
- Designing ultra-fast DL/DTL-based OPM method truly proper for real-time implementations, speeding-up GSNR estimation 1e6 and 1e9 times compared with the well-known closed-form and integral-form EGN models, respectively.
- Proposing DTL-based OPM in FMF transmission, having superior capabilities of fast remodeling and data resource reservation enabling the possibility for real-time implementations.
- Providing a comprehensive investigation over DL/DTL-based OPM for FMF by presenting performance analysis considering scenarios, preparing complexity analysis considering well-known conventional methods, investigating complexity-performance trade-off between proposed algorithms and well-known conventional methods, and discussing the practical aspect of the proposed techniques.

The rest of this paper is organized as follows; Section 2 describes the system model, and Section 3 presents the DL and DTL-based OPM methods. Simulation results and discussions are provided in Sections 4 and 5, respectively. Section 6 is the conclusion of this work.

2. System model

We consider signal transmission in the FMF link described by Fig. 1 which is composed of N_s spans with ideal optical amplifiers at the end of each span for compensating attenuation which in turn produces ASE noise [1,17]. The transmitted signal is a multiplexing of D spatial modes and N_{ch} wavelength channels. The signal propagation suffers from linear effects such as modal dispersion, chromatic dispersion, and linear coupling, as well as nonlinear effects including Kerr-based nonlinear effect and nonlinear coupling [1,17]. An ideal de-multiplexer is used at the receiver accompanied by MIMO DSP to compensate linear effects [1,17]. The nonlinear phase rotation is recovered by carrier phase estimator (CPE) [4,48]. Based on the well-known EGN model, the received signal after CPE can be modeled as a summation of the transmitted signal and ASE and NLI noise [4]. Therefore, the GSNR of nth channel and pth mode after CPE can be formulated as [4]

$$GSNR_{n,p} = \frac{P_{n,p}}{\sigma^2_{ASE,n,p} + \sigma^2_{NLI,n,p}}, \tag{1}$$

where $P_{n,p}$ is the launched power of nth channel and pth mode, $\sigma^2_{ASE_{n,p}}$ and $\sigma^2_{NLI,n,p}$ respectively are ASE and NLI noise variances of nth channel and pth mode [4].

3. Proposed DL and DTL-based OPM methods

The proposed DL-based OPM (Fig. 2(a)) and DTL-based OPM (Fig. 2(b)) methods are composed of a DNN (Fig. 2(c)) with N_f input neurons where N_f is number of features, N_{hid} hidden layers each with N_{neu} hidden neurons, and one output neuron. Therefore, the DNN has $L = N_{hid} + 2$ layers, the input vector of the lth layer, $r_{l-1}; l = \{1, 2, \ldots, L\}$, is multiplied by a weight matrix, added by a bias vector, and passed through an activation function and a dropout layer. The GSNR calculated by the EGN model is the true GSNR (label), $GSNR^{n,p}_{true}$, and the DNN output represents the predicted GSNR, $GSNR^{n,p}_{pred}$. The aim is to adjust the DNN hyperparameters such that $GSNR^{n,p}_{pred}$ becomes as close as possible to $GSNR^{n,p}_{true}$. The DNN input–output mapping function can be expressed by

$$r_L = f(r_0; \boldsymbol{\theta}), \tag{2}$$

where $f(\cdot)$ is the mapping function, r_0 is DNN input vector, r_L is DNN output vector, $\boldsymbol{\theta} = \{\theta_1, \ldots, \theta_L\}$ is the hyperparameters with

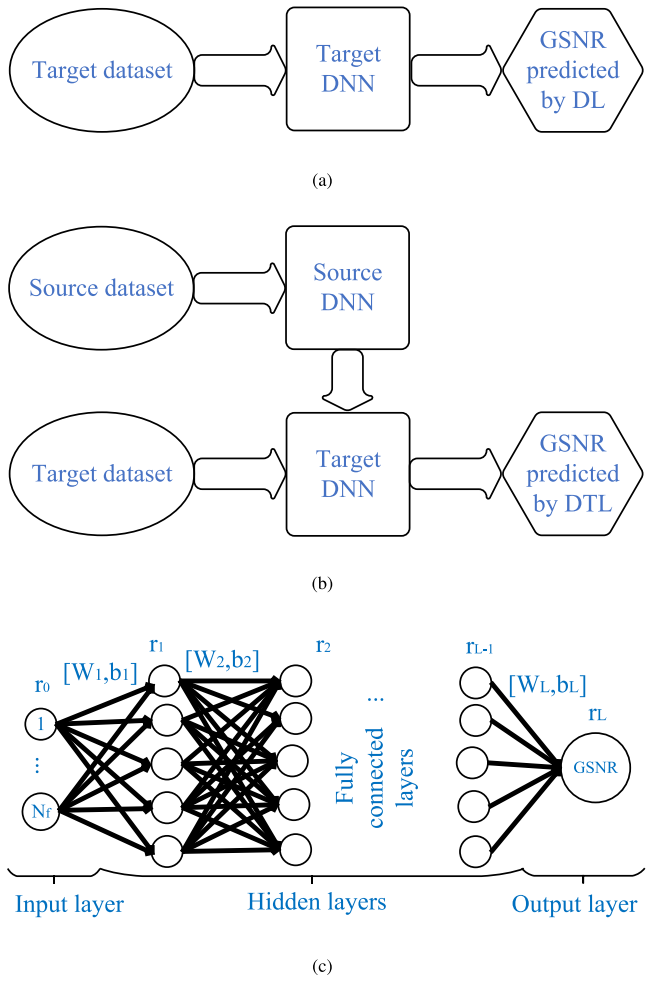

Fig. 2. Structure of proposed (a) DL-based, (b) DTL-based OPM methods, and (c) target/source DNN.

$\theta_l = \{W_l, b_l\}$, and W_l and b_l are weight matrix and bias vector of lth layer, respectively. Thus the following relationship can be expressed for the lth layer

$$r_l = f_l(r_{l-1}; \theta_l) = \alpha_l(W_l r_{l-1} + b_l), \tag{3}$$

where $f_l(\cdot)$ and $\alpha_l(\cdot)$ are respectively the mapping function and activation function of lth layer. The following relationship can be written between $GSNR^{n,p}_{pred}$ and $\boldsymbol{\theta}$

$$\begin{aligned} GSNR^{n,p}_{pred} &= f_L(\ldots(f_2(f_1(y;\theta_1);\theta_2)\ldots);\theta_L) \\ &= \alpha_L(\ldots\alpha_2(W_2(\alpha_1(W_1 r_0 + b_1) + b2)\ldots)). \end{aligned} \tag{4}$$

We define the following loss function for training the DNN

$$L(\boldsymbol{\theta}) = \frac{1}{k}\sum_{k=1}^{K} l^k(GSNR^{true,k}_{n,p}, GSNR^{pred,k}_{n,p}), \tag{5}$$

where K is the batch size, $l^k(.,.)$ is the loss function, and superscript k refers to the kth batch of the training dataset. $\boldsymbol{\theta}$ can be obtained by minimizing the loss function. The most prevalent methods for this purpose are stochastic gradient descent algorithms among which the Adam algorithm is a well-known and widely used [49]. The Adam updates $\boldsymbol{\theta}$ iteratively using the following formulation

$$\boldsymbol{\theta}^{(j+1)} = \boldsymbol{\theta}^{(j)} - \eta \nabla_{\boldsymbol{\theta}} \hat{L}(\boldsymbol{\theta}^{(j)}), \tag{6}$$

Table 2
Considered system and link parameters.

Coefficient	Value
Number of channels	66
Symbol rate	64 GBaud
Channel bandwidth	75 GHz
Span length	Uniformly distributed between 80 and 120 km
Coupling length	80 km
Number of spans	1–8
Center frequency	193.5 THz

where η is the learning rate, j is the iteration number, and $\nabla_{\boldsymbol{\theta}}\hat{L}(\cdot)$ is the estimated gradient of $\hat{L}(\cdot)$ which is fed back as an updating guide in each iteration [49].

Note that in DL-based OPM we train and test the DNN based on the target dataset while in DTL-based OPM the DNN training is based on the source dataset and then the trained DNN weights and biases are used as the starting point for DNN training and testing based on target dataset.

4. Simulation results

In this section, we first explain dataset generation and DNN hyperparameter tuning. Then, we provide the performance and complexity analysis of the proposed DL/DTL-based OPM method. The simulations are done in the Python environment, scikit-learn library [50].

4.1. Dataset generation

FMF system and link configuration: A Large dataset is required for proper training DL/DTL-based algorithm for OPM in FMF. However, gathering large field datasets is very hard considering different number of spans and span lengths. Furthermore, generating a large synthetic dataset using the SSFM method is impractical considering the whole C-band and few modes [52]. We should mention that our accessible Intel Xeon CPU with 32 cores and 64 GB RAM limits SSFM simulation to 9 channels (0.45 THz bandwidth) and 3 modes. Therefore, we generate source and target datasets synthetically based on the EGN model considering system and link parameters described by Table 2. We utilize the whole C-band with 5 THz bandwidth, 66 channels working at 193.5 THz center frequency with 64 GB*aud* symbol rate and 75 GHz channel spacing (28% overhead). The standard polarization multiplexed quadrature phase-shift keying modulation is employed for each channel and mode. The signal propagation is on 1 to 8 spans with span length uniformly distributed between 80 to 120 km. At each span, an ideal amplifier with 5 dB noise figure compensates attenuation. Both weak and strong linear coupling regimes are considered with a coupling length of 80 km. The parameter setting for source and target datasets is presented in Table 3. In the source dataset, we consider 0 dBm launched power, 1 spatial mode (LP01) propagating in fiber type 1. In the target dataset, the launched power is uniformly distributed between −5 dBm to 5 dBm, and 3 spatial modes are considered propagating in fiber type 2. One can consider the source domain as a simplified scenario of the target domain. The nonlinear coupling coefficients for fiber type 2 are presented in Table 4. The nonlinearity coefficient, attenuation, modal dispersion, and chromatic dispersion for fiber types 1 and 2 are presented in Table 5.

Feature set: The proposed DL/DTL-based OPM method aims to predict the GSNR values calculated by the EGN model. The channel-mode under test indices, number of spans, span length, and launched power of channel-mode under test are parameters affecting the GSNR calculation while using the EGN model,

Table 3
Parameter setting of source and target datasets.

Parameter	Source dataset	Target dataset
Power	0 dBm	Uniformly distributed between −5 and 5 dBm
Fiber type	Type 1	Type 2
Number of modes	1(LP01)	3(LP01, LP11a, LP11b)

Table 4
Nonlinear coupling coefficient between pth and qth mode for fiber type 2 [51].

pq	LP01	LP11a	LP11b
LP01	0.73	0.36	0.36
LP11a	0.36	0.55	0.18
LP11b	0.36	0.18	0.55

therefore, it is useful to consider them as features. For dataset generation, we provide three "for loops" for sweeping different spans (8 spans), modes (1 mode in source and 3 modes in target dataset), and channels (66 channels). At each iteration, we randomly select span length and launched power, and repeat the whole procedure 300 times for SMF and 100 times for FMF to generate a $300 \times 8 \times 1 \times 66 = 158400$ point source dataset and a $100 \times 8 \times 3 \times 66 = 158400$ point target dataset.

Feature space: The channel index includes integer values between 1 to 66, and can take 66 different values, the mode index has integer values between 1 and 3, thus it can take 3 values. The number of spans is compromised between 1 to 8 with 8 integer values. The span length is uniformly distributed between 80 to 120 km (with 1 m granularity) which provides infinite values. The launched power of the channel and mode under test is uniformly distributed between −5 dBm to 5 dBm and imposes infinite values. Hence, the feature space sweeps limited dimensions each with an unlimited area. Therefore, utilizing a look-up table generated by pre-calculated values using the EGN model instead of DL/DTL models is impractical. Since, in our case, calculating each value by the EGN model takes almost half an hour, and even a small change in system/link (see [1–4]) which makes even a huge look-up table not functional. Besides, a look-up table can only cover the limited available cases while DL/DTL aims to cover the non-available cases by learning the information of available cases.

4.2. Tuned DNN structure

The DNN hyperparameter tuning is done based on instructions provided by [49]. The tuned DNN structure is composed of an input layer with 5 neurons, 2 hidden layers with 5 and 500 neurons, and an output layer with 1 neuron. The linear activation function is employed at the input and output layers. The rectified linear unit (Relu) activation function is used at hidden layers, as Relu avoids the gradient saturation problem. Adam optimizer is employed with a learning rate of 0.001. To prevent overfitting, initial normalization, and batch normalization are established [53, 54].

4.3. Performance analysis

Fig. 3 depicts RMSE of $GSNR_{pred}$ versus the number of epochs for DL and DTL-based OPM methods, considering 2^{11} samples. DTL-based OPM method converges after a few epochs which shows efficient knowledge transfer between source and target domains. DTL and DL-based OPM methods converge at 50 and 250 epochs, respectively. Therefore, the DTL-based OPM reduces the required training epochs by around 5 times in comparison with DL-based OPM.

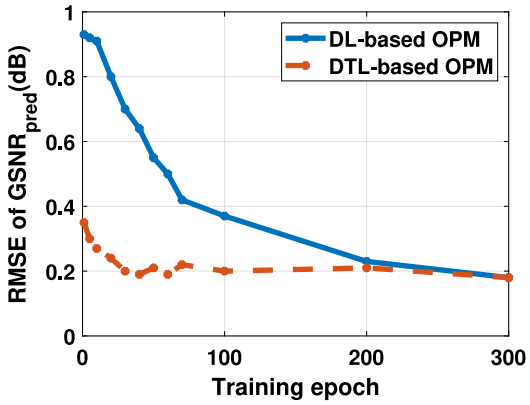

Fig. 3. RMSE of $GSNR_{pred}$ versus the number of epochs for DL and DTL-based OPM methods.

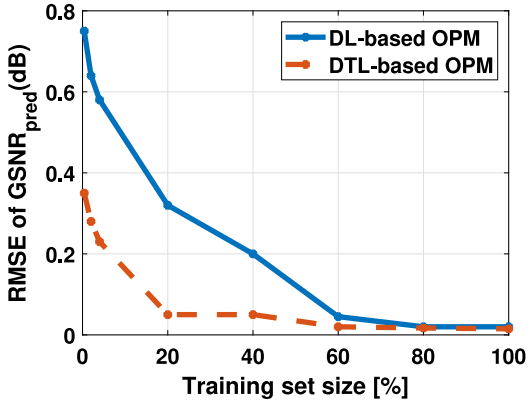

Fig. 4. RMSE of $GSNR_{pred}$ versus training size for DL and DTL-based OPM methods.

We also compare the required training dataset size for the DL and DTL-based OPM methods in Fig. 4 in terms of RMSE of $GSNR_{pred}$ versus training size. The RMSE reduces by increasing the training dataset size in both methods, however, DTL-based OPM has a faster steep. DL and DTL-based OPM methods converge to the same RMSE, since they have the same DNN structure and learn the same information while training. DTL and DL-based OPM methods converge to 0.02 dB RMSE of $GSNR_{pred}$ with 25% and 75% of training dataset size, respectively. Therefore, the DTL-based OPM method reduces the required dataset size 3 times in comparison with DL-based OPM which in turn decreases the training time.

In the case of source and target dataset independence, the knowledge taken from the source model has no impact on the learning of the target model. In other words, retraining and transfer learning would have the same results. However, the FMF channel is relatively stable or slowly varied which makes source and target datasets to be partially correlated [1,17]. As a result (and as seen in Fig. 4), utilizing the knowledge taken from the source model can speed up the training based on the target. In fact, DTL-based OPM learns the target model using a superior trained starting point which is beneficial for fast remodeling [47].

Table 5
Nonlinearity coefficient, attenuation, modal dispersion, and chromatic dispersion for fiber types 1 [6] and 2 [51].

	Type 1	Type 2		
Parameter	LP01	LP01	LP11a	LP11b
Nonlinearity coefficient [1/watt/km]	1.3	1	1	1
Attenuation [dB/km]	0.226	0.2	0.2	0.2
Modal Dispersion [ps/km]	0	−0.29	−0.66	−0.66
Chromatic dispersion [ps^2/km]	31.9	28.3	28.2	28.2

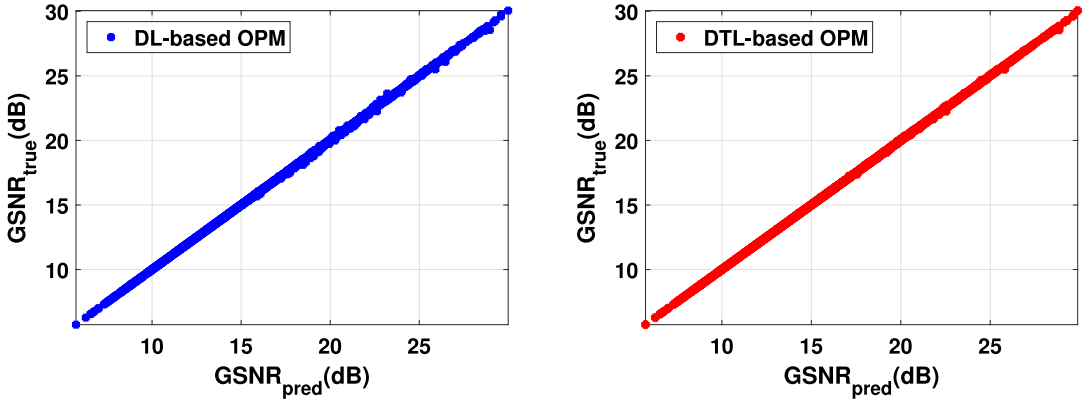

Fig. 5. Scatterplot of $GSNR_{pred}$ and $GSNR_{true}$ for (a) DL-based and (b) DTL-based OPM methods.

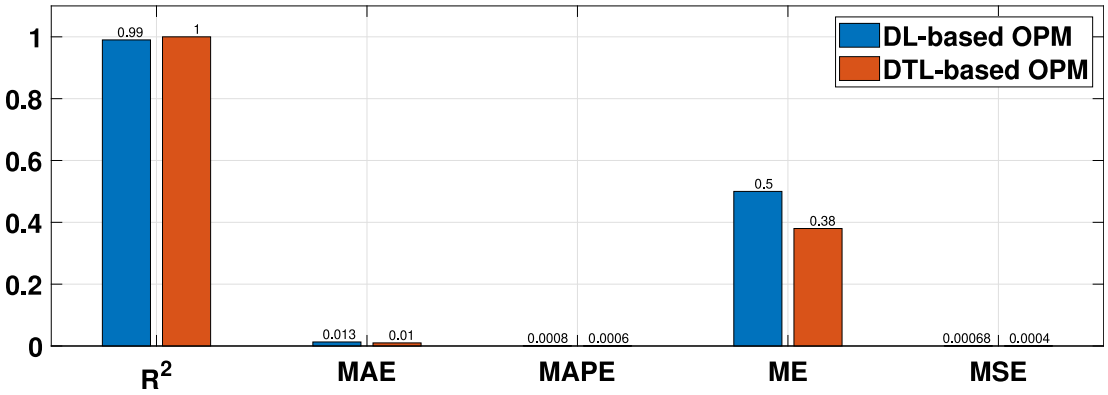

Fig. 6. R^2, MAE (in dB), MAPE, ME (in dB), and MSE values for DTL-based QoT estimation method.

Figs. 5(a) and 5(b) respectively demonstrate scatterplots of $GSNR_{pred}$ and $GSNR_{true}$ for DL and DTL-based OPM methods, considering 200 epochs. The scatterplots of both methods are propagated along the $x = y$ line which indicates good performance. DTL-based OPM provides a denser scatterplot, and a better performance, compared with DL-based OPM.

Fig. 6 demonstrates R^2, mean absolute error (MAE), mean absolute percentage error (MAPE), maximum error (ME), and MSE, as defined in [50], for DL/DTL-based OPM, considering 200 epochs. The R^2 value measures how well a statistical model can predict the outcome, as seen, DL/DTL-based OPM method can predict quite well. The MAE measures the mean of the absolute differences between the predicted and reference outputs while the MAPE measures the mean of the absolute differences between the predicted and reference outputs divided by the reference output. A little better value for ME is obtained for DLT compared with DL. The obtained low MSE value is indicative of a proper GSNR estimation in the DL/DTL-based OPM method.

Fig. 7(a) illustrates cumulative distribution function (CDF) of $|\Delta GSNR|$ with $\Delta GSNR = GSNR_{pred} - GSNR_{true}$ for DL and DTL-based OPM methods, considering 200 epochs. The CDF of $|\Delta GSNR|$ is 99% below 0.2 dB and 0.1 dB for DL and DTL-based OPM, respectively which indicates that the proposed OPM methods properly predict the GSNR. Fig. 7(b) describes the probability density function (pdf) and CDF of $\Delta GSNR$ for the DL/DTL-based OPM approach, considering 200 epochs. The quite small mean and variance values verify the prediction performance of the DL/DTL-based OPM method. DTL-based OPM provides a smaller mean and variance compared with DL-based OPM. Besides, DTL-based OPM NLI noise overestimation is more than DL-based OPM which shows that DTL-based OPM is on the safer side.

4.4. Complexity analysis

Table 6 shows the complexity analysis of DL/DTL-based OPM method, SSFM, integral-form EGN, and GN models, as well as closed-form EGN and GN models. The training of the DL/DTL-based OPM method is done offline and once, therefore, we do not need to consider training complexity. Moreover, we take into account only the forward propagation, since the backward propagation happens just while training. The presented complexity of the DL/DTL-based OPM in Table 6 is equal to the number of

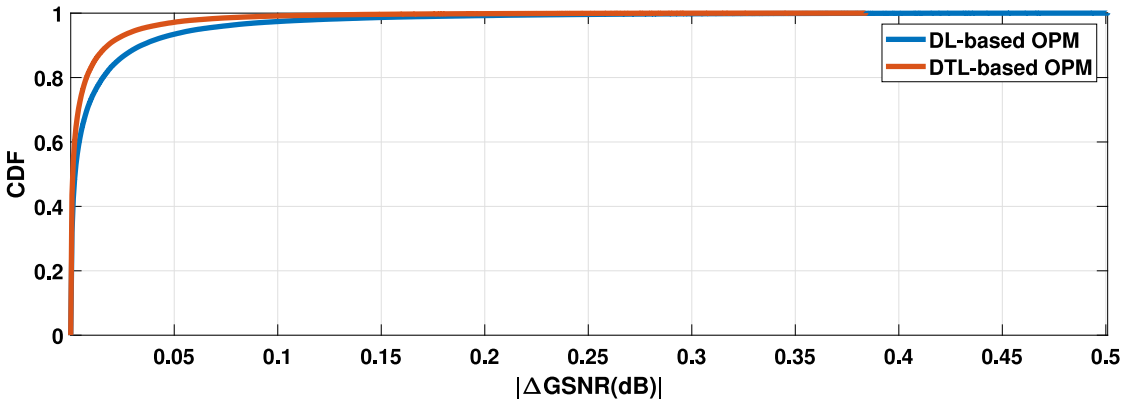

(a)

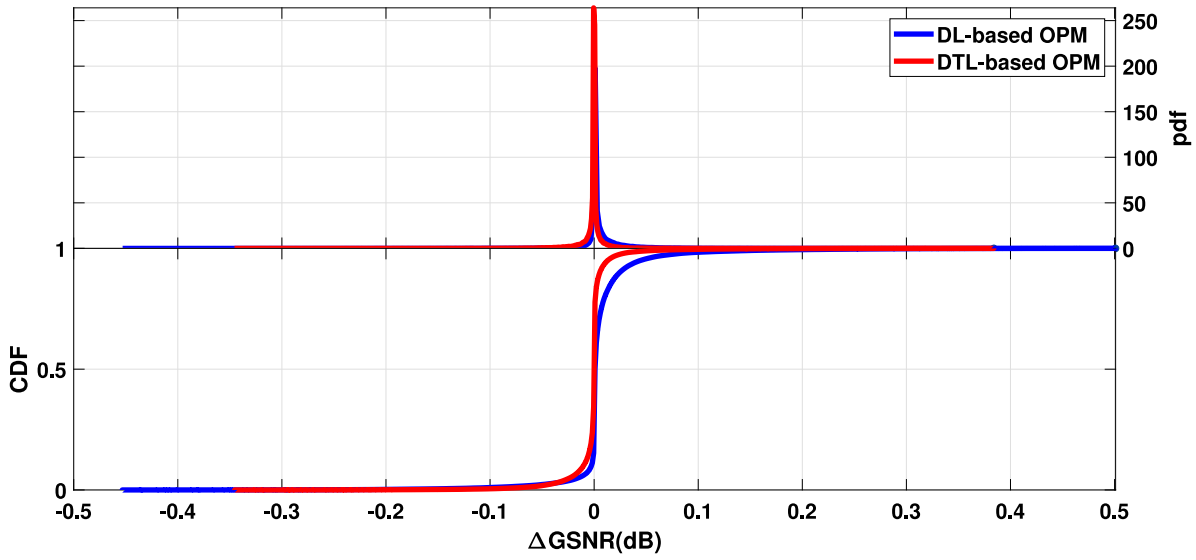

(b)

Fig. 7. (a) CDF of $|\Delta GSNR|$ and (b) pdf and CDF of $\Delta GSNR$ for DL and DTL-based OPM methods.

Table 6
Computational complexity of proposed DL/DTL-based OPM method, SSFM, integral-form EGN, and GN models, as well as closed-form EGN and GN models.

Methods	Number of multiplications	Number of summations
DL/DTL-based OPM	$(N_{neu}(N_{hid}N_{neu}+N_f+1))/2$	$(N_{neu}(N_{hid}(N_{neu}+1)+N_f+1))/2$
SSFM simulation	$(N_{step}N_s)(8DN_{sym}log(DN_{sym})+6DN_{sym}+2n_1+1)+(4DN_{sym}log(DN_{sym})+4DN_{sym}+2n_1)$	$(N_{step}N_s)(8DN_{sym}log(DN_{sym})+2DN_{sym}+n_1+2)+(2DN_{sym}log(DN_{sym})+4DN_{sym}+n_1)$
Integral-form EGN model	$8Dn_2n_3n_4(2n_1+4)$	$8Dn_2n_3n_4(n_1+6)$
Integral-form GN model	$2Dn_2n_3n_4(2n_1+3)$	$2Dn_2n_3n_4(n_1+5)$
Closed-form EGN model	$4DN_{ch}(8n_1+6)+2$	$4DN_{ch}(4n_1+4)$
Closed-form GN model	$DN_{ch}(8n_1+5)+2$	$DN_{ch}(4n_1+3)$

multiplications and summations of the DNN which is composed of an input layer with N_f neurons, N_{hid} hidden layers each with N_{neu} hidden neurons, and an output layer with 1 neuron. The SSFM simulation includes several processing such as MDM and WDM multiplexer and de-multiplexer, EDFAs (at each span), and dispersion compensation (at the receiver). Note that each span has N_{step} steps, and at each step, there are two blocks implementing FMF linear and nonlinear effects. The transmitted WDM signal dimension is $2DN_{sym}$ with N_{sym} as the number of symbols of each channel-mode, thus the fast Fourier transform (FFT)/inverse FFT related to dispersion implementation/removal has $2DN_{sym}\log(2DN_{sym})$ multiplications/summations. The $exp(x) = \sum_{i=0}^{n_1} x_i/i!$ term can be calculated using $2n_1$ multiplications and n_1 summations where n_1 is an integer, the larger n_1 the better accuracy. The complexity analysis of the integral-form EGN and GN models are based on equations (25) of [4] and (17) of [2], respectively. The integral-form EGN and GN models respectively include four and one 3D integration which for numerically calculating, n_2, n_3 and n_4 points with identical distances should be considered for the first, second and third dimensions. By so doing, $n_2 \times n_3 \times n_4$ small 3D areas appear over which taking a 3D summation is equivalent to the 3D integration over the main 3D area. The larger n_2, n_3, and n_4 the better accuracy can be obtained. The complexity analysis of closed-form EGN and

GN models are based on equations (6) of [1] and (13) of [3], respectively. The complexity orders of the DL/DTL-based OPM method, integral-form EGN/GN model, and closed-form EGN/GN, are respectively $O(N_{neu}^2)$, $O(n_1n_2n_3n_4)$, and $O(n_1)$. Considering the fact that $n_1n_2n_3n_4 \gg n_1 \gg N_{neu}^2$, the DL/DTL-based OPM method provides much less complexity in comparison with the other methods.

The difference between the closed-form and integral-form GN model is about 0.2 dB as reported by [55]. However, the integral/closed-form GN model considers Gaussian modulation for the transmitted signal which results in around 1 dB overestimation of NLI noise power in practical applications with modulation formats such as quadrature phase shift keying [4]. Besides, the closed-form GN/EGN model is only applicable to rectangular-shaped Nyquist WDM with channel spacing close to symbol rate [1,3]. However, DTL-based OPM provides $\Delta GSNR$ respectively below 0.1 dB, 0.05 dB, and 0.03 dB in 99%, 95%, and 90% of trials without any specific system/link assumption, considering a very wide range of system/link configurations. We remark that the GSNR estimation times of the DL/DTL-based OPM method, closed-form GN/EGN, and integral-form GN/EGN are about $1e-6$ s, 1 s, and $1e3$ s, respectively. In other words, DL/DTL-based OPM method speeds up GSNR estimation $1e6$ and $1e9$ times compared with integral-form GN/EGN and closed-form GN/EGN models, respectively.

5. Discussions

The use of DL/DTL-based OPM can provide many benefits either to the current or the future adaptive and autonomous FMF networks. Here, we discuss some notes on the applicability aspect of this technology and the associated enablers.

- **Real-time applicability**: DL/DTL-based OPM helps in the real-time utilization of information about FMF network status and results in designing proactive FMF networks using constantly adaptive models. DL/DTL-based OPM predicts the fault occurrence probability even if FMF system/link parameters are varying, thus ensuring a reliable operation which is crucial in applications such as medicine wherein diagnosis and treatment times should be short enough. FMF network can monitor performance changes, send feedback to adapt the transmission parameters automatically, reduce downtime and increase network availability. Therefore, DL/DTL-based OPM can be helpful in future FMF networks which are dynamic and flexible with adaptable system/link parameters regarding customer requirements and link status.
- **Security guarantee**: There is no accurate model for physical layer impairments under attacks while DL/DTL-based OPM can continuously monitor optical parameters in regard to any attack and be helpful for recognizing and detecting unpredictable and detrimental attacks targeting FMF networks.
- **Intelligent resource utilization**: Building intelligent nodes with the OPM function helps to use FMF network resources efficiently. To achieve the maximum of the said efficiency, the OPM functions should be able to improve their performance and efficiency over time as in DL/DTL-based OPM. It is difficult to provide a closed-form formulation in FMF EONs which handle a large number of tunable parameters. However, DL/DTL-based OPM can deal with complex nonlinear relationships and result in better resource utilization.
- **Cost effectiveness**: Although DL/DTL-based OPM deployment in FMF networks is along with building and integrating costs, the so-called re-learning ability enhances cost-effectiveness compared to conventional approaches. In a cost-limited OPM scenario, only simple hardware components can be deployed and partial signal features can be obtained for monitoring of parameters. As a consequence, the input–output mapping of parameters would be intractable from underlying physics/mathematics. However, DL/DTL-based OPM is the real-time acquisition of information about impairments and is not affected by this. Typically, OPM collects parameters at various points, increasing the number of monitors and costs. Therefore, it is required to deploy OPM in the proper locations. In this regard, DL/DTL-based OPM can be used to learn the mapping between the system/link parameters and the signal properties.

6. Conclusions

In this paper, we have proposed and demonstrated DL and DTL-based methods for OPM in FMF. The proposed DL and DTL-based OPM methods guarantee the GSNR estimation RMSE of 0.02 dB. We have done the feasibility test of the proposed DTL-based OPM method considering a transfer from SMF to FMF with completely different fiber types and power regimes. Results show the robustness of the DTL-based OPM method. In addition, the proposed DTL-based OPM reduces the training dataset size and epoch respectively around 3 and 5 times in comparison with the proposed DL-based OPM.

CRediT authorship contribution statement

M.A. Amirabadi: Conception and design of study, Writing – original draft, Writing – review & editing. **M.H. Kahaei:** Conception and design of study, Writing – original draft, Writing – review & editing. **S.A. Nezamalhosseini:** Conception and design of study, Writing – original draft, Writing – review & editing.

Declaration of competing interest

All authors have participated in (a) conception and design, or analysis and interpretation of the data; (b) drafting the article or revising it critically for important intellectual content; and (c) approval of the final version.

This manuscript has not been submitted to, nor is under review at, another journal or other publishing venue.

The authors have no affiliation with any organization with a direct or indirect financial interest in the subject matter discussed in the manuscript

Data availability

The authors do not have permission to share data.

Acknowledgment

All authors approved the version of the manuscript to be published.

References

[1] M.A. Amirabadi, M.H. Kahaei, S.A. Nezamalhosseini, F. Arpanaei, A. Carena, Closed-form EGN model for FMF systems, in: Asia Communications and Photonics Conference, 2021, pp. T4A–33.

[2] M.A. Amirabadi, M.H. Kahaei, S.A. Nezamalhosseini, Lawrence R. Chen, Improving MDM-WDM optical network performance via optimal power allocation using Gaussian noise model, Opt. Fiber Technol., Mater. Devices Syst. 75 (2023) 103187.

[3] M.A. Amirabadi, M.H. Kahaei, S.A. Nezamalhosseini, L.R. Chen, Optimal power allocation in nonlinear MDM-WDM systems using Gaussian noise model, IET Optoelectron. (2022).

[4] M.A. Amirabadi, M.H. Kahaei, S.A. Nezamalhosseini, L.R. Chen, Joint power and gain allocation in MDM-WDM optical communication networks based on extended Gaussian noise model, IEEE Access (2022).
[5] C. Koebele, M. Salsi, L. Milord, R. Ryf, C. Bolle, P. Sillard, S. Bigo, G. Charlet, 40km transmission of five mode division multiplexed data streams at 100Gb/s with low MIMO-DSP complexity, in: European Conference and Exposition on Optical Communications, 2011, pp. 1–3.
[6] S. Mumtaz, R.J. Essiambre, G.P. Agrawal, Nonlinear propagation in multimode and multi-core fibers: Generalization of the Manakov equations, J. Lightwave Technol. 31 (3) (2012) 398–406.
[7] G. Rademacher, K. Petermann, Nonlinear Gaussian noise model for multimode fibers with space-division multiplexing, J. Lightwave Technol. 34 (9) (2016) 2280–2287.
[8] A. Mecozzi, C. Antonelli, M. Shtaif, Coupled Manakov equations in multimode fibers with strongly coupled groups of modes, Opt. Express 20 (21) (2012) 23436–23441.
[9] A.E. Elfiqi, A.A. Ali, Z.A. El-Sahn, K. Kato, H.M. Shalaby, Theoretical analysis of long-haul systems adopting mode-division multiplexing, Opt. Commun. 445 (2019) 10–18.
[10] J. Li, Z. Wu, D. Ge, J. Zhu, Y. Tian, Y. Zhang, J. Yu, Z. Li, Z. Chen, Y. He, Weakly-coupled mode division multiplexing over conventional multi-mode fiber with intensity modulation and direct detection, Front. Optoelectron. 12 (1) (2019) 31–40.
[11] P. Sillard, Few-mode-fiber developments and applications, in: 2018 23rd Opto-Electronics and Communications Conference, OECC, 2018, pp. 1–2.
[12] B. Inan, B. Spinnler, F. Ferreira, D. van den Borne, A. Lobato, S. Adhikari, V. Sleiffer, M. Kuschnerov, N. Hanik, S. Jansen, DSP complexity of mode-division multiplexed receivers, Opt. Express 20 (10) (2012) 10859–10869.
[13] G. Rademacher, S. Warm, K. Petermann, Nonlinear interaction in differential mode delay managed mode-division multiplexed transmission systems, Opt. Express 23 (1) (2015) 55–60.
[14] G. Rademacher, R.S. Luis, B.J. Puttnam, H. Furukawa, R. Maruyama, K. Aikawa, Y. Awaji, N. Wada, Investigation of inter-modal four-wave mixing for nonlinear signal processing in few-mode fibers, IEEE Photonics Technol. Lett. 30 (17) (2018) 1527–1530.
[15] F. Ye, S. Warm, K. Petermann, Differential mode delay management in spliced multimode fiber transmission systems, in: Optical Fiber Communication Conference and Exposition and the National Fiber Optic Engineers Conference, 2013, pp. 1–3.
[16] G. Rademacher, R.S. Luís, B.J. Puttnam, R. Maruyama, K. Aikawa, Y. Awaji, H. Furukawa, K. Petermann, N. Wada, Investigation of intermodal nonlinear signal distortions in few-mode fiber transmission, J. Lightwave Technol. 37 (4) (2019) 1273–1279.
[17] G. Rademacher, F. Schmidt, K. Petermann, Optimum capacity utilization in space-division multiplexed transmission systems with multimode fibers, in: 42nd European Conference on Optical Communication, ECOC 2016, 2016, pp. 1–3.
[18] D. Kroushkov, G. Rademacher, K. Petermann, Cross mode modulation in multimode fibers, Opt. Lett. 38 (10) (2013) 1642–1644.
[19] A.D. Ellis, N. Mac Suibhne, F.C.G. Gunning, S. Sygletos, Expressions for the nonlinear transmission performance of multi-mode optical fiber, Opt. Express 21 (19) (2013) 22834–22846.
[20] Z. Dong, A.P.T. Lau, C. Lu, OSNR monitoring for QPSK and 16-QAM systems in presence of fiber nonlinearities for digital coherent receivers, Opt. Express 20 (17) (2012) 19520–19534.
[21] P. Poggiolini, The GN model of non-linear propagation in uncompensated coherent optical systems, J. Lightwave Technol. 30 (24) (2012) 3857–3879.
[22] P. Poggiolini, Y. Jiang, A. Carena, F. Forghieri, A simple and accurate closed-form EGN model formula, 2015, arXiv preprint arXiv:1503.04132.
[23] A. Carena, G. Bosco, V. Curri, Y. Jiang, P. Poggiolini, F. Forghieri, EGN model of non-linear fiber propagation, Opt. Express 22 (13) (2014) 16335–16362.
[24] P. Poggiolini, G. Bosco, A. Carena, V. Curri, Y. Jiang, F. Forghieri, The GN-model of fiber non-linear propagation and its applications, J. Lightwave Technol. 32 (4) (2013) 694–721.
[25] D. Azzimonti, C. Rottondi, A. Giusti, M. Tornatore, A. Bianco, Comparison of domain adaptation and active learning techniques for quality of transmission estimation with small-sized training datasets, J. Opt. Commun. Netw. 13 (1) (2021) A56–A66.
[26] P.J. Freire, D. Abode, J.E. Prilepsky, N. Costa, B. Spinnler, A. Napoli, S.K. Turitsyn, Transfer learning for neural networks-based equalizers in coherent optical systems, J. Lightwave Technol. 39 (21) (2021) 6733–6745.
[27] D. Azzimonti, C. Rottondi, M. Tornatore, Reducing probes for quality of transmission estimation in optical networks with active learning, J. Opt. Commun. Netw. 12 (1) (2020) A38–A48.
[28] D. Azzimonti, C. Rottondi, A. Giusti, M. Tornatore, A. Bianco, Active vs transfer learning approaches for QoT estimation with small training datasets, in: Optical Fiber Communication Conference, 2020, pp. M4E–1.
[29] C. Rottondi, R. di Marino, M. Nava, A. Giusti, A. Bianco, On the benefits of domain adaptation techniques for quality of transmission estimation in optical networks, J. Opt. Commun. Netw. 13 (1) (2021) A34–A43.
[30] Y. Cheng, W. Zhang, S. Fu, M. Tang, D. Liu, Transfer learning simplified multi-task deep neural network for PDM-64QAM optical performance monitoring, Opt. Express 28 (5) (2020) 7607–7617.
[31] Y. Xu, D. Wang, M. Zhang, X. Zhou, Z. Zhang, J. Li, Y. Zhu, P. Xie, N. Paerhati, Deep transfer learning based multi-impairment diagnosis for PAM-4 optical communication systems, in: 2019 18th International Conference on Optical Communications and Networks, ICOCN, 2019, pp. 1–3.
[32] F.N. Khan, T.S.R. Shen, Y. Zhou, A.P.T. Lau, C. Lu, Optical performance monitoring using artificial neural networks trained with empirical moments of asynchronously sampled signal amplitudes, IEEE Photonics Technol. Lett. 24 (12) (2012) 982–984.
[33] S. Yang, L. Yang, F. Luo, B. Li, X. Wang, Y. Du, D. Liu, Joint fiber nonlinear noise estimation, OSNR estimation and modulation format identification based on asynchronous complex histograms and deep learning for digital coherent receivers, Sensors 21 (2) (2021) 380.
[34] A.S. Kashi, Q. Zhuge, J.C. Cartledge, A. Borowiec, D. Charlton, C. Laperle, M. O'Sullivan, Fiber nonlinear noise-to-signal ratio monitoring using artificial neural networks, in: 2017 European Conference on Optical Communication, ECOC, 2017, pp. 1–3.
[35] L. Xia, J. Zhang, Y. Song, Q. Zhang, X. Li, K. Qiu, Physical layer abstraction utilizing OSNR montioring based on deep neural network, in: Asia Communications and Photonics Conference, 2018, pp. M3D–4.
[36] F.N. Khan, K. Zhong, W.H. Al-Arashi, C. Yu, C. Lu, A.P.T. Lau, Modulation format identification in coherent receivers using deep machine learning, IEEE Photonics Technol. Lett. 28 (17) (2016) 1886–1889.
[37] J. Du, T. Yang, X. Chen, J. Chai, Y. Zhao, S. Shi, A CNN-based cost-effective modulation format identification scheme by low-bandwidth direct detecting and low rate sampling for elastic optical networks, Opt. Commun. 471 (2020) 126007.
[38] F. Shen, J. Zhou, Z. Huang, L. Li, Going deeper into OSNR estimation with CNN, Photonics 8 (9) (2021) 402.
[39] H. Lv, X. Zhou, J. Huo, J. Yuan, Joint OSNR monitoring and modulation format identification on signal amplitude histograms using convolutional neural network, Opt. Fiber Technol., Mater. Devices Syst. 61 (2021) 102455.
[40] Z. Wang, A. Yang, P. Guo, P. He, OSNR and nonlinear noise power estimation for optical fiber communication systems using LSTM based deep learning technique, Opt. Express 26 (16) (2018) 21346–21357.
[41] Y. Zhou, Z. Yang, Q. Sun, C. Yu, C. Yu, An artificial intelligence model based on multi-step feature engineering and deep attention network for optical network performance monitoring, Optik 273 (2023) 170443.
[42] L. Xia, J. Zhang, S. Hu, M. Zhu, Y. Song, K. Qiu, Transfer learning assisted deep neural network for OSNR estimation, Opt. Express 27 (14) (2019) 19398–19406.
[43] W.S. Saif, A.M. Ragheb, H.E. Seleem, T.A. Alshawi, S.A. Alshebeili, Modulation format identification in mode division multiplexed optical networks, IEEE Access 7 (2019) 156207–156216.
[44] W.S. Saif, A.M. Ragheb, M.A. Esmail, M. Marey, S.A. Alshebeili, Machine learning based low-cost optical performance monitoring in mode division multiplexed optical networks, Photonics 9 (2) (2022) 73.
[45] W.S. Saif, A.M. Ragheb, T.A. Alshawi, S.A. Alshebeili, Optical performance monitoring in mode division multiplexed optical networks, J. Lightwave Technol. 39 (2) (2021) 491–504.
[46] X. Zhu, B. Liu, X. Zhu, J. Ren, R. Ullah, Y. Mao, X. Wu, S. Chen, M. Li, Y. Bai, Optical performance monitoring via domain adversarial adaptation in few-mode fiber, Opt. Commun. 510 (2022) 127933.
[47] X. Zhu, B. Liu, X. Zhu, J. Ren, R. Ullah, Y. Mao, X. Wu, M. Li, S. Chen, Y. Bai, Transfer learning assisted convolutional neural networks for modulation format recognition in few-mode fibers, Opt. Express 29 (22) (2021) 36953–36963.
[48] P. Serena, C. Lasagni, A. Bononi, The enhanced Gaussian noise model extended to polarization-dependent loss, J. Lightwave Technol. 38 (20) (2020) 5685–5694.
[49] M.A. Amirabadi, M.H. Kahaei, S.A. Nezamalhosseini, Novel suboptimal approaches for hyperparameter tuning of deep neural network [under the shelf of optical communication], Phys. Commun. 41 (2020) 101057.
[50] F. Pedregosa, G. Varoquaux, A. Gramfort, V. Michel, B. Thirion, O. Grisel, M. Blondel, P. Prettenhofer, R. Weiss, V. Dubourg, J. Vanderplas, Scikit-learn: ML in Python, J. ML Res. 12 (2011) 2825–2830.
[51] F.M. Ferreira, C.S. Costa, S. Sygletos, A.D. Ellis, Overcoming degradation in spatial multiplexing systems with stochastic nonlinear impairments, Sci. Rep. 8 (1) (2018) 1–10.

[52] M.A. Amirabadi, M.H. Kahaei, S.A. Nezamalhosseini, A. Carena, Deep learning regression vs. Classification for QoT estimation in SMF and FMF links, in: ICOP, 2022.
[53] M.A. Amirabadi, M.H. Kahaei, S.A. Nezamalhosseini, F. Arpanaei, A. Carena, Deep neural network-based QoT estimation for SMF and FMF links, J. Lightwave Technol. (2022).
[54] M.A. Amirabadi, M.H. Kahaei, S.A. Nezamalhosseini, A. Carena, Deep learning for QoT estimation in SMF and FMF links, in: ACP/IPOC, 2022.
[55] D. Semrau, R.I. Killey, P. Bayvel, A closed-form approximation of the Gaussian noise model in the presence of inter-channel stimulated Raman scattering, J. Lightwave Technol. 37 (9) (2019) 1924–1936.

Mohammad Ali Amirabadi was born in Zahedan, Iran, in 1993. He received the B.Sc. degree in Optics & Laser Engineering from Malek-e-Ashtar University of Technology, Isfahan, Iran, in 2015, and the M.Sc. degree in Communication Engineering from Iran University of Science and Technology, Tehran, Iran in 2017. Now he is studying Ph.D. in Communication Engineering in Iran University of Science and Technology, Tehran, Iran. His research interests include Multimode Fiber Optic Communication, Free Space Optical Communication, and Deep Learning.

Mohammad Hossein Kahaei received the B.Sc. degree in electrical engineering from Isfahan University of Technology, Isfahan, Iran, in 1986, the M.Sc. degree in adaptive signal processing from the University of the Ryukyus, Okinawa, Japan, in 1994, and the Ph.D. degree in signal processing from Queensland University of Technology, Brisbane, Australia, in 1998. Since 1999, he has been with the School of Electrical Engineering, Iran University of Science and Technology, Tehran, Iran, where he is currently an Associate Professor and the Head of Signal and System Modeling laboratory. His research interests include array signal processing with primary emphasis on compressed sensing, sparse optimization problems, data science, localization, tracking, DOA estimation, blind source separation, and wireless sensor networks.

S. Alireza Nezamalhosseini received the B.Sc. degree in electrical engineering from Amirkabir University of Technology, Tehran, Iran, in 2006, and the M.Sc. and Ph.D. degrees in electrical engineering from Sharif University of Technology (SUT), Tehran, Iran, in 2008 and 2013, respectively. He is currently an assistant professor at Iran University of Science and Technology (IUST), Tehran. His research interests include underwater wireless optical communications, mode-division multiplexing in optical fibers, and visible light communications.